Est. 1984

ORIENTAL JOURNAL OF CHEMISTRY
An International Open Access, Peer Reviewed Research Journal

www.orientjchem.org

ISSN: 0970-020 X
CODEN: OJCHEG
2021, Vol. 37, No.(1):
Pg. 71-79

Wood-industrial Waste Material as a Potential Sorbent for the Removal of Pb^{+2} and Co^{+2} from Mono and Binary Aquatic Metal Solutions

KSHIPRA NIMODIA[1], ARUNA SOLANKI[1], LAXMI KUNWAR CHAUHAN[1], AJAY KUMAR GOSWAMI[1] and PRABHAT KUMAR BAROLIYA[1]*

Department of Chemistry, Mohanlal Sukhadia University, Udaipur-313001, Rajasthan, India.
*Corresponding author E-mail: prabhatkbaroliya@mlsu.ac.in

http://dx.doi.org/10.13005/ojc/370109

(Received: August 20, 2020; Accepted: February 19, 2021)

ABSTRACT

In this research, the practical feasibility of sawdust waste products from wood-processing industries was evaluated for the elimination of Pb^{+2} and Co^{+2} metal ions from mono and binary aquatic solutions. The batch method was used to achieve optimum conditions of including the amount of sorbent, pH, process time, and concentration of metal ions. The absorptive cycle reported maximum removal of lead and cobalt within pH range 6.0 at an initial concentration of 10 mg L^{-1}. Kinetics data collected during the adsorption of both metals is better represented in a pseudo-second-order layout. The equilibrium of adsorption is based on the concept of Langmuir adsorption layout. Thermodynamic parameters demonstrated the feasibility, spontaneity, and endothermic character of heavy metal sorption. The sorption of metal ions was verified by instrumental experiments for example scanning electron microscope (SEM), energy dispersive X-ray spectrometry (EDX), and Fourier transform infrared spectroscopy (FTIR). Thus, sawdust can be an effective material for removing Pb^{+2} and Co^{+2} ions from aquatic solutions.

Keywords: Heavy metals, Sawdust, Sorption, Sorption isotherms, Sorption kinetics.

INTRODUCTION

Heavy metal contamination is a fast increasing environmental issue across the world with the extension to manufacturing practices. The commercial usage of metals raises the accumulation of metals in air, water, and soil. Trace metals are common in the atmosphere and can reach the food chain from the atmosphere[1]. The presence of heavy metals in aqueous solutions above a certain limit poses a significant danger to the atmosphere due to their non-degradability and toxicity. Lead is one of the four heavy metals that may inflict significant adverse effects on human wellbeing, resulting in damage to the lungs, immune system, digestive organs, liver, and brain. Lead is commonly used in the manufacture of automotive batteries, pigments, paints, plumbing, weapons, ceramics industries, etc. Large amounts of lead are commonly present in the soil, groundwater, and residual waters attributable to these industries[2,3].

Exposure to elevated amounts of cobalt has also been linked with negative health effects such as neurotoxicological conditions, human genotoxicity, and as well as persistent cancer[4]. The most popular therapies for metals recovery from water and wastewater include electrolysis, ion exchange, chemical deposition and reverse osmosis[5,6]. Nonetheless, each of these approaches has disadvantages, such as costly activity and chemical sludge production. Therefore, it is necessary to develop more reliable and cost-effective processes[7,8]. Adsorption is an ideal method to treat polluted water, with advantages including reduced costs, increased flexibility, energy effectiveness, operating simplicity, and reliability in decreasing heavy metal ion concentration to very low levels[9].

During recent years, sorption has acquired more creditability as a technologically feasible and economic operation for the removal of toxic metals from wastewater[10]. Sawdust is a useful material, as it is created as waste material in vast amounts at the sawmill. The sawdust comprises mainly of lignin, cellulose and hemicellulose, readily adsorbs heavy metal ion impurities present in waste water[11,12]. Such lignocellulosic materials often have ionic charge and thus have an ion exchange capacity[13,14]. In the work we described, the sorption potential of sawdust in both mono and binary-component systems for the elimination of Pb^{+2} and Co^{+2} ions. The study considered various sorption parameters affecting sorption behavior in mono and binary systems, including pH influence, a dose of adsorbent and the processing time, initial concentration, and temperature.

To obtain the best model that fits the sorption system, the isothermal and kinetic parameters were also determined.

MATERIAL AND METHODS

Materials

The sawdust was collected from the nearby wood furniture industry used as adsorbent. It was washed many times with deionized water to ensure that total impurities on the surface were eliminated. The washed material was cured for 24 h in an oven at of 100°C and then sieved to get a particle of the mean size of 0.63 mm and is deposited before use. All chemical compounds were analytical standards. Heavy metal ion stock solutions (HMI) (1000 mg L^{-1}) were derived from $Pb(NO_3)_2$ and $Co(NO_3)_2 \bullet 6H_2O$. For the sorption tests, different required dilutions were made with a concentrating stock solution.

Characterizations

The FTIR study was performed to identify the surface functional units of sawdust before and after Pb^{+2} and Co^{+2} ions adsorption. The sample morphologies and sizes were defined by scanning electron microscope (SEM JSM-6100 JEOL, Japan, SAIF Chandigarh, India) fitted with an energy-dispersive analyzer of X-ray (EDX) to conduct a detailed analysis of the sample.

Batch sorption Tests and Investigation

Batch sorption tests for mono metal ion systems were conducted to explore the impact of heavy metal sorption by sawdust in 250 mL conical flasks containing 1 g of sawdust with 100 mL of Pb^{+2} and Co^{+2} solutions (1000 mg L^{-1}). It was sealed and stirred on a mechanical stirrer at 120 rpm at ambient temperature. The pH-dependent sorption study was carried out in addition to a larger pH ranging (pH 2–8), controlled via 0.1 M HNO_3 and NaOH solutions. The sorbent dosage influence was examined at a constant pH (6 ± 0.1) with a variable dose (0.4-1.8 mg g^{-1}) at ambient temperature. Sorption kinetics is conducted by monitoring the time of contact of the metal solutions and the sorbent at various time periods (10-60 minutes). For the analysis of the isotherm of sorption, the initial metal concentration ranges between 10-100 mg L^{-1}. The influence of temperature was recorded across the temperature range of 25–65°C for the sorption tests. Upon sorption, the mixtures were passed via filter paper Whatman No. 1, and the metal content within each flask was measured using atomic absorption spectrophotometer (Elico SL168). The binary metal analysis was performed to explore the influence of both metal ions coexistence on the overall sorption potential of the sorbent. Batch experiments were followed the same as used in the mono metal ion system. Throughout the experiment, although the primary concentration of one metal ion in the mixture was 10-100 mg L^{-1}, the other metal ion concentration stayed unchanged at a steady pH of 6.0. The quantity of heavy metal adsorbed to the sorbent was estimated using the following equations[15]:

$$q_e = \frac{V\,(C_o - C_e)}{w} \quad (1)$$

$$\text{Removal efficiency} = \frac{C_o - C_e}{C_o} \times 100 \quad (2)$$

Here qe (mg g^{-1}) is the quantity of metal sorbed at equilibrium condition, the volume V (mL) is of the aqueous medium, C_0, and C_e (mg L^{-1}) are the initial and equilibrium metal ion concentration, and W (mg) is the sorbent weight.

RESULT AND DISCUSSION

Characterizations of Sorbents

Sawdust particles have been examined by SEM-EDX to analyze the morphological structure and the chemical composition of the sorbent. The SEM pictures of the NSD (natural sawdust), Pb^{+2} loaded, and Co^{+2}-loaded sawdust was demonstrated by Fig. 1 (a), (b), and (c). The NSD surface (Fig. 1(a)) is abundant with an uneven surface with a porous composition which is ideal for the trapping and adsorbing metal ions into certain pores. Surface morphology changes appear to arise when Pb^{+2} and Co^{+2} ions associate with donor functional units on sawdust, as seen in Fig. 1 (b) and (c), separately. The chemical analysis of sorbent before and after metal sorption is represented in Fig. 2 (a), (b), and (c) of the EDX (Analyzer sequence for Hitachi SU8010). The appearance of C, O, Al, S, Na, and Ca as natural species on the adsorbent be seen from Fig. 2 (a) of the sorbent before metal uptake. Yet, according to Fig. 2 (b and c), the strong peaks of metal ions reflecting the Pb^{+2} and Co^{+2} sorption on the surfaces of the sorbent. The FTIR spectra of sawdust are seen in Fig. 3 (a), (b), and (c) before and after the metal ion sorption. The broad absorbance peaks of approximately 3311 cm^{-1} suggest the existence of hydroxyl groups that imply the prevalence of phenols and alcohols in Fig. 3 (a) of NSD which, is shifted to 3345 and 3616 cm^{-1} after Pb^{+2} and Co^{+2} uptake, separately (Fig. 3 b and c). The field between 3005 and 2881 cm-1 indicated the existence of the –CH and $–CH_2$ aliphatic framework. This value is moved to 2978 cm^{-1} for Pb^{+2} and 2976 cm^{-1} for Co^{+2}. The existence of a carbonyl group on the sawdust surface was confirmed by the occurrence of a typical peak for C = O at ~1736 cm^{-1}, which is wider and sharper after metal sorption. The peak of about 1647 cm^{-1} is related to the C=O (amide band primarily a stretching band), which changes to 1689 cm^{-1}. The small peaks at 1508 cm^{-1} were linked to C=C aromatic stretching, and the tiny peak around ~1229 cm^{-1} C-OH stretching vibration of carboxylic acids and phenols which, is also shifted after metal uptake. FTIR results have shown that –OH is mainly involved in metal sorption on sawdust inside the carboxylic, phenolic, and amide groups. The sorbent shows a series of peaks of absorption, which represent the complex structure of sorbent.

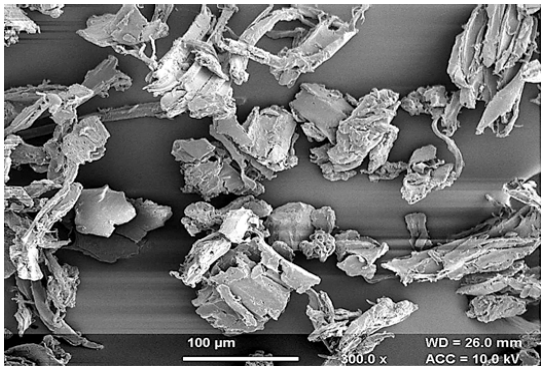

(a)

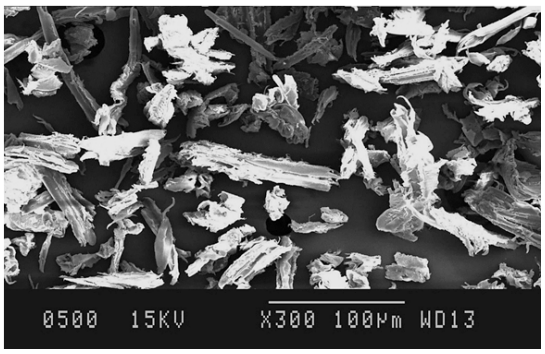

(b)

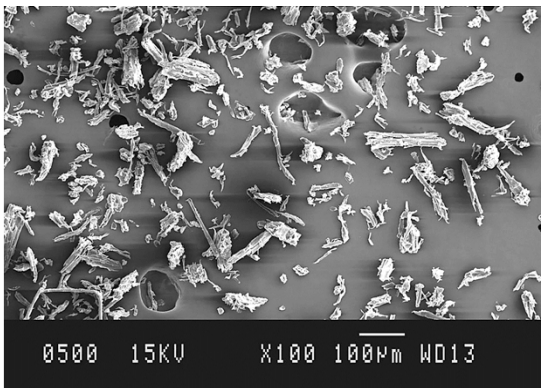

(c)

Fig. 1 (a). Scanning Electron Microstructure (SEM) displays natural sawdust morphology; (b) SEM picture of sawdust after Pb^{+2} ion sorption; (c) SEM picture of sawdust after Co^{+2} ion sorption

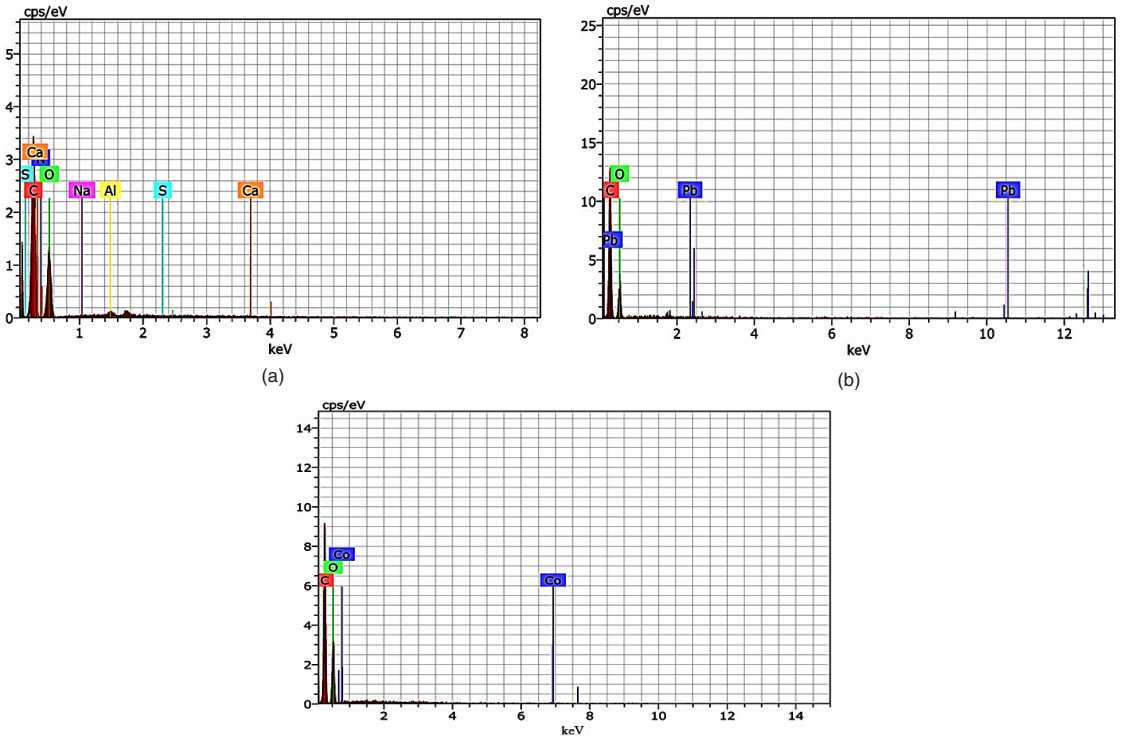

Fig. 2 (a). EDX spectrum of natural sawdust; (b) EDX spectrum of sawdust after Pb(II) ion sorption; (c) EDX spectrum of sawdust after Co(II) ion sorption

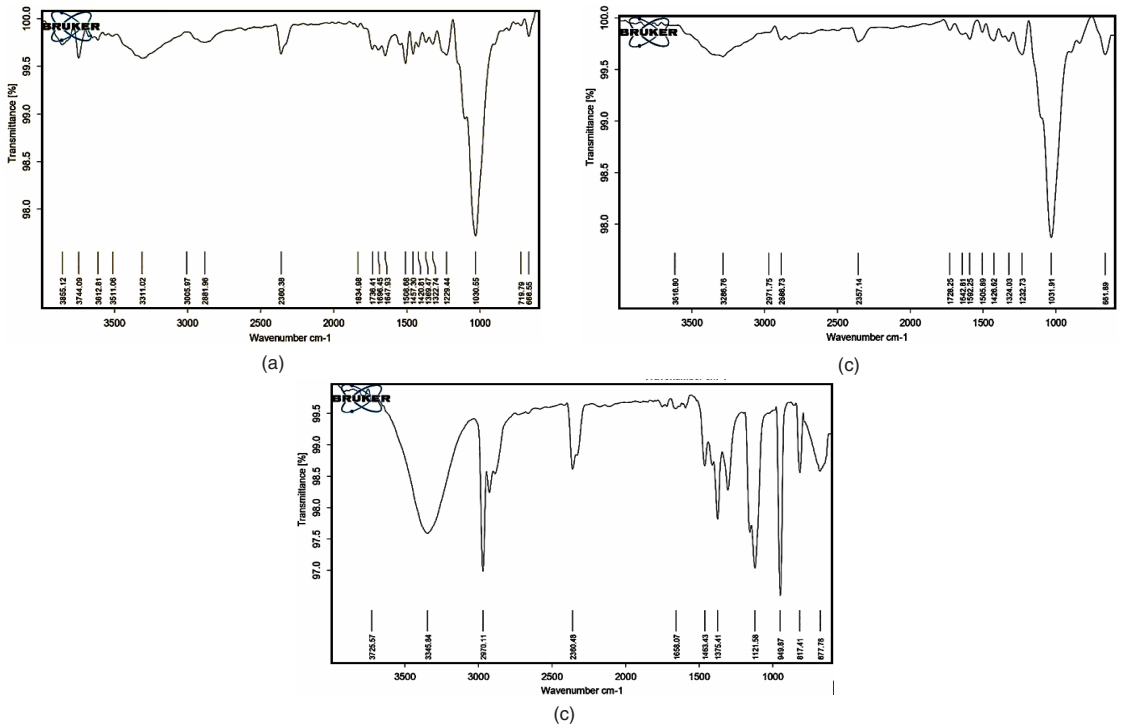

Fig. 3 (a). FTIR spectrum of natural sawdust; (b) FTIR spectrum of after Pb^{+2} ion sorption; (c) FTIR spectrum of after Co^{+2} ion sorption

Influence of sorbent Dose and pH

The sorbent dose influence was investigated, holding the other experimental conditions constant. It was observed that there was a rapid increase in percent removal of both metal ions with a dosage raise from 0.2 g to 1.0 g, as depicted in Fig. 4, credited to the higher availability of sites to bind or surface areas at higher sorbent concentrations[16]. The optimum sorbent dosage has therefore been selected at 1.0 g L^{-1}. An additional increase in the mass of sorbents above 1.0 g L^{-1} did not make a remarkable improvement in the removal percentage of the two metal ions.

The pH is one of the key factors for governing heavy metal ion sorption[17,18]. To examine the pH impact on the elimination of Pb^{+2} and Co^{+2} ions the pH was changed to 2-8. The experimental findings indicate that metals have a high removal rate up to pH 6.0. A significant improvement in the efficiency of removal of Pb^{+2} and Co^{+2} was found in addition to a rise in pH from 2.0 to 6.0 and a slight decline at pH > 6.0 (Fig. 5). Conversely, at higher pH, the H^+ concentrations were smaller, so the adsorbent surface functional groups deprotonated[19], and the sorption intensity did not increase anymore.

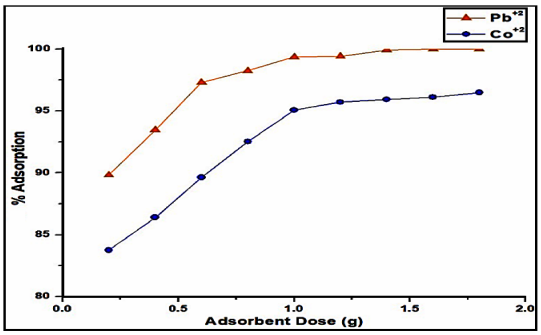

Fig. 4. Impact of sorbent dose on the sorption of Pb^{+2} and Co^{+2} ions (initial Conc.-10 mg L^{-1}; temp-298K and pH-6.00)

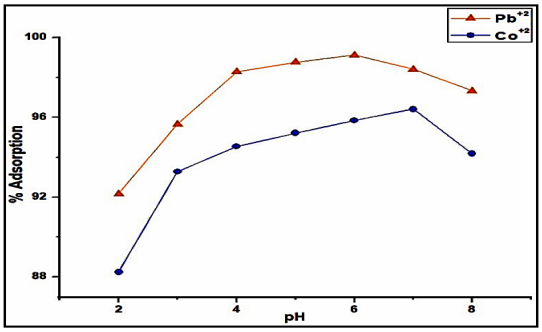

Fig. 5. Impact of pH on the sorption of Pb^{+2} and Co^{+2} ions (initial conc.-10 mg L^{-1}; temp298K and adsorbent dosage-1.0 g L^{-1})

Sorption Isotherms

In the isotherm analysis, the commonly preferred models Langmuir and Freundlich were tested to provide an insight inside the heavy metal sorption on sawdust at constant temperature conditions. The isotherm experiment was conducted at initial metal concentrations varying from 10 to 100 mg L^{-1}. The Freundlich parameters including n (surface heterogeneity factor) and K_f (Freundlich Constant) were obtained from the slope and intercept of the plot of log q_e versus log C_e, as seen in Fig. 6(a) and Table 1. The Langmuir parameter q_m (mg g^{-1}) defined the magnitude of maximum sorption, and K_L (L mg^{-1}) is the Langmuir constant referring to the free sorption energy. They were calculated by the slope and intercept of the graph between C_e/q_e and C_e (Fig. 6(b) and Table 1). This may be inferred that the Langmuir model best matched the results obtained from the Freundlich model by evaluating the associated correlation coefficient (R^2) values. The correlation coefficient (R^2) values for both metals in the Langmuir model, which are quite similar to 1, are almost ideal. From Langmuir isotherm, the highest q_m (maximum sorption capacity) values were shown by Pb^{+2} than Co^{+2} in both mono and binary metal systems. It was supposed that the greater the value of K_L, the greater the affinity of the sorbent sensitivity to the metal sorbed[20]. For both metals, the K_L value indicates that in the relative order from the maximum to the lowest of the Co(Co–Pb)<Co(II)<Pb(Pb-Co)<Pb(II), the tendency of the sawdust to adsorb the same trend as that seen for R^2 and q_m.

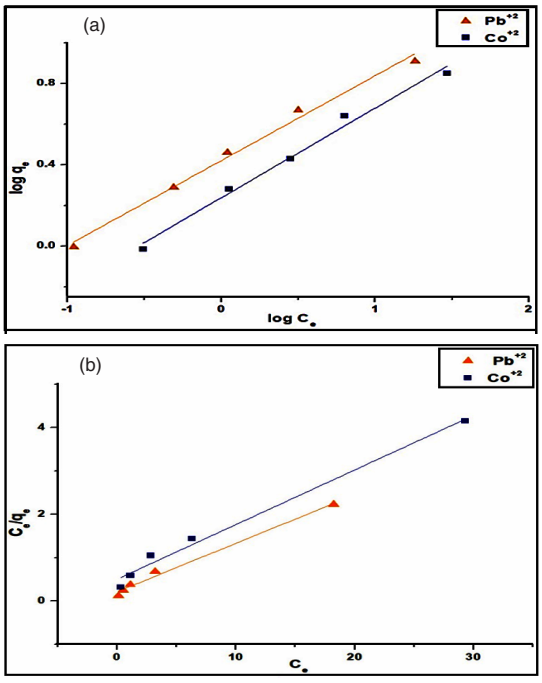

Fig. 6 (a). Graph of Freundlich isotherm for the sorption of Pb^{+2} and Co^{+2} metal ions at 298 K; (b) Graph of Langmuir isotherm for the sorption of Pb^{+2} and Co^{+2} metal ions at 298 K

Table 1: Isotherm variables for the sorption of ions onto sawdust in mono and binary component frameworks at 30°C

Metal ions System	Langmuir			Freundlich		
	q_m (mg g^{-1})	K_L(b) (L mg^{-1})	R^2	1/n	K_f (mg g^{-1})	R^2
Pb^{+2}	9.09	0.516	0.99	0.417	2.63	0.98
Co^{+2}	8	0.247	0.99	0.48	1.72	0.98
Pb^{+2} with appearance of Co^{+2}	7.35	0.109	0.96	0.49	0.959	0.99
Co^{+2} with appearance of Pb^{+2}	6.67	0.069	0.99	0.63	0.58	0.99

Sorption Kinetics

Sorption kinetics is an essential aspect that offers knowledge regarding the efficacy of the adsorption cycle. To achieve the kinetics of sorption of Pb and Co for sawdust, Lagergren's first order and pseudo-second-order equations were used (Figure 7 a and b)[21].

The Lagergren's pseudo-first-order kinetic model rate expression is as[22]:

$$\log(q_e - q) = \log q_e - (k_{ads}/2.303)\, t \qquad (3)$$

q_e and q_t are the quantity of metal ion adsorbed at the condition of equilibrium and at time t, respectively (mg/g), and k_{ads} is the equilibrium constant of the pseudo-first-order reaction. The quantities sorbed at equilibrium condition (q_e) (mg g^{-1}) and k_{ads}(min^{-1}) is the pseudo-first-order sorption rate constant obtained by the graph of log (q_e-q_t) vs t (Figure 7 (a)).

The pseudo-second-order for sorption kinetics can thus be written as follows[23]:

$$\frac{t}{q} = 1/k_2 q_e^2 + t \qquad (4)$$

Here k_2 (g mg^{-1} min^{-1}) is the constant of the pseudo-second-order equation. The reaction rate equilibrium constant k_2 (g mg^{-1} min^{-1}) and the equilibrium adsorbed amounts (q_e) (mg g^{-1}) is gained from the slope and intercept of linear plots between t/q_t and t (Fig. 7(b)) for sorption of metal ions. The values of kinetic significance and the associated coefficients of correlation are described in Table 2. The high R^2 values revealed that pseudo-second-order equations are more suited to data than those of Lagergren's kinetic expression of pseudo-first-order[24]. The kinetic data obtained indicate that Pb^{+2} and Co^{+2} sorption adopted second-order-kinetic model, based on the presumption that sorption could be a step of the rate determining[25].

Prediction of a rate-defining step is an essential consideration for recognization in the design of the sorption cycle. In the case of a solid-liquid phase of sorption, the transition of the solute is typically categorized by external mass transfer (boundary level diffusion) or diffusion of the intraparticle, or both[26]. An intraparticle diffusion was used to describe the pathway involved in the sorption cycle. The rate constant of intraparticle diffusion is expressed as:

$$q_t = k_d\, t^{1/2} \qquad (5)$$

For the following equation, q_t is the metal ions quantity sorbed (mg g^{-1}) at time t, $t^{1/2}$ defines the square root of the different mixing time and K_d is constant. The q_t vs. $t^{1/2}$ plot as seen in Fig. 7 (c) corresponds to the specific stages of sorption. The initial part is connected to diffusion of the boundary layer and the second linear section reflects the diffusion of the intraparticle. Both regions of the plot show that surface sorption and intraparticle diffusion is needed for the metal sorption on sawdust. The intraparticle diffusion coefficient is measured by the slope of the second linear part of the plot (k_d). Table 2 presents the measured coefficient data. Whereas, the intercept of the plot shows the impact of the boundary layer. The bigger the intercept, the more surface sorption contribution was found[27].

Table 2: Pseudo-first-order, pseudo-second-order and intra-particle diffusion variables for the sorption of metal ions on sawdust at 30°C

Metals	Pseudo first order		Pseudo second order		Intra-particle diffusion	
	K_{ads}(min^{-1})	R^2	K^2 (g mg^{-1} min^{-1})	R^2	K_d ($min^{1/2}$)	R
Pb^{+2}	0.0299	0.97	0.005	0.99	0.13	0.99
Co^{+2}	0.046	0.91	0.007	0.97	0.12	0.98

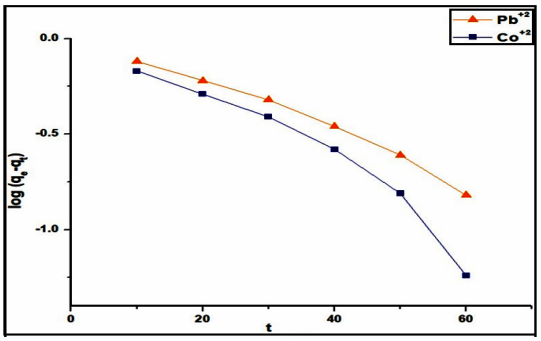

(a)

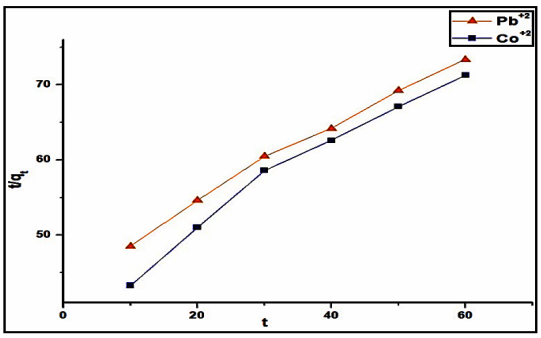

(b)

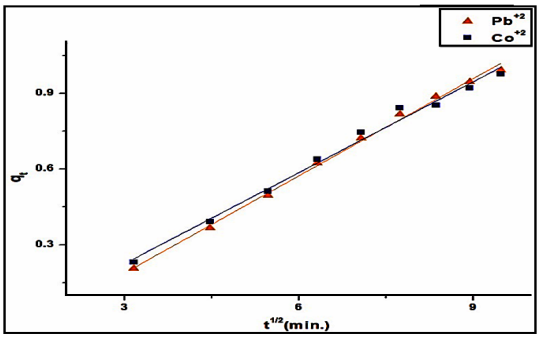

(c)

Fig. 7 (a). Graph of pseudo-first-order kinetic for the sorption of Pb^{+2} and Co^{+2} metal ions at 298 K; (b) Graph of pseudo-second-order kinetic for the sorption of Pb^{+2} and Co^{+2} metal ions at 298 K. (c) Plots of amount adsorbed vs. square root of time for Pb^{+2} and Co^{+2} metal ion sorption

Sorption Thermodynamics

The thermodynamic nature of Pb^{+2} and Co^{+2} sorption was explored by estimating various thermodynamic variables like Gibbs free energy (ΔG^{o}), entropy (ΔS^{o}), and enthalpy (ΔH^{o}). The parameters listed above were evaluated by the following equation[28,29]:

$$\Delta G^{\circ} = -RT \ln K_D \quad (6)$$

$$\ln K_D = \Delta S^{\circ}/R - \Delta H^{\circ}/RT \quad (7)$$

R is the uniform gas constant (8.314 J mol^{-1} K^{-1}), T is the temperature (K) and K_D represents standard equation constant. However, ΔH^{o} and ΔS^{o} quantities were determined increasing the slope, and ln K_D vs T^{-1} (Fig. 8) plot intercept respectively. Table 3 displays thermodynamic parameters. For P_b as well as for C_o all the values of ΔH^{o} were positive. This can be shown that heavy metal sorption on sawdust was an endothermic process[30]. Positive ΔS° values may also be induced by a difference in the sorbent composition, which supports the sensitivity of the sorbent to the adsorbed substrate (Pb^{+2} and Co^{+2}) and the adsorbent cycle stability[31-33]. The negative values of ΔG^{o} indicate that sorption of ions is a spontaneous action and is thermodynamically favorable. The Gibbs free energy (G) values are small and negative and decrease with rising temperatures[34].

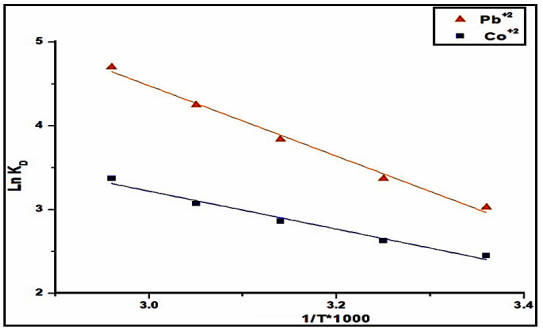

Fig. 8. Graph of Ln k_D vs. T^{-1} (K) for Pb^{+2} and Co^{+2} ions

Table 3: Thermodynamic constants for the sorption of ions on sawdust at 30°C

Metal Ions	T(K)	ΔG^{o} (KJ mol^{-1})	ΔH^{o} (KJ mol^{-1})	ΔS^{o} (KJ $mol^{-1}K^{-1}$)	R (KJ $mol^{-1}K^{-1}$)
	298	-7.4			
	308	-8.82			
Pb^{+2}	318	-10.24	34.92	0.142	8.314
	328	-11.66			
	338	-13.08			
	298	-6.01			
	308	-6.84			
Co^{+2}	318	-7.68	18.79	0.083	8.314
	328	-8.51			
	338	-9.34			

Competitive sorption

Table 4 displays findings of mono and binary sorption of Pb^{+2} and Co^{+2} ions and indicates that the ion sorption ability for Pb^{+2} was significantly greater than that of Co^{+2} ions. When the metal concentration rises from 10 to 100 mg L^{-1}, the sorption capacity of sawdust is also raised for Pb^{+2} ions and Co^{+2} ions. The initial concentration of metal supplies the driving forces required to overcome resistance between media and sawdust to the exchange of Pb^{+2} or Co^{+2} ions. The table indicates an average sorption yield of 20 mg L^{-1} (10 mg L^{-1} each) is needed to be equivalent to 91.70, while the average experiment yield for both metal ions found 85.00. Fig. 9 (a) and (b) specifically indicated that the sorption yield of Pb^{+2} was higher than that of Co^{+2} ions towards sorbent. The variation of Pb^{+2} and Co^{+2} in the sorption was attributed to their ionic radii differences which were 1.75 and 2.25A°, respectively. The results indicated that a decrease in the hydrated ion radius in aqueous solutions would increase the capacity for biomass sorption[35]. The competitive sorption of metal ions was reported to be lower than the non-competitive sorption. Results indicate that the multi-component system (Pb^{+2} and Co^{+2}) will demonstrate competitive and antagonistic sorption.

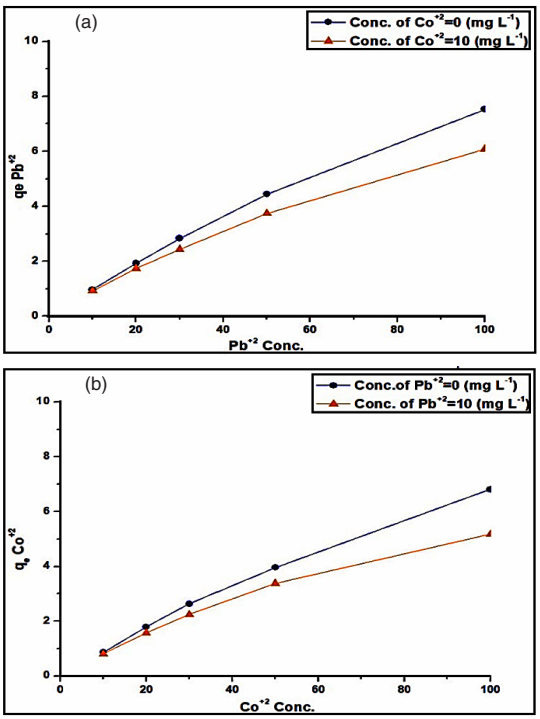

Fig. 9 (a). Comparison of the equilibrium sorption of Pb^{+2} in the presence of Co^{+2} on sawdust (dose-1.0; pH-6.0;temp-298 K); (b) Comparison of the equilibriumsorption of Co^{+2} in the presence of Pb^{+2} onsawdust (dose-1.0; pH-6.0; temp-298 K)

Table 4: Impact of competitive sorption of Pb^{+2} and Co^{+2} ions onto sawdust at various ion concentrations

Pb conc. (mg L^{-1})	qe Pb (mg g^{-1})	% Ad.	Initial Co Conc. (mg L^{-1})	Total % Ad.
10	0.97	97.2	0	97.2
20	1.92	96.15	0	96.15
30	2.83	94.37	0	94.37
50	4.44	88.74	0	88.74
100	7.53	75.31	0	75.31
0	0.00	0.00	10.0	86.2
10	0.92	91.6	10.0	87.25
20	1.74	86.8	10.0	81.85
30	2.44	81.23	10.0	75.87
50	3.74	74.7	10.0	69.05
100	6.08	60.79	10.0	56.5
Co conc. (mg L^{-1})	qe Co (mg g^{-1})	% Ad.	Initial Pb Conc. (mg L^{-1})	Total % Ad.
10	0.86	86.2	0	86.2
20	1.79	89.65	0	89.65
30	2.63	87.73	0	87.73
50	3.96	79.16	0	79.16
100	6.81	68.14	0	68.14
0	0.00	0.00	10.0	97.2
10	0.81	81.3	10.0	82.75
20	1.57	78.4	10.0	80.05
30	2.24	74.63	10.0	76.17
50	3.38	67.52	10.0	68.56
100	5.17	51.68	10.0	56.54

ACKNOWLEDGMENT

The authors are grateful to the Coordination Chemistry Lab, Department of Chemistry, MLSU University, Udaipur, India. Thanks for characterizations (SEM and EDX) to the SAIF Chandigarh, India.

Conflict of Interest

The authors declare that there is no conflict of interest.

REFERENCES

1. Harshala, P.; Shreeram, J.; Niyoti, S.; Arvind, L.; Sarma, U.S.; Sudersan; *Process Biochem.*, **2009**, *41*, 605–615.
2. Emsley, J.; Nature's Building Blocks: an A-z Guide to the Elements. Oxford University Press, USA., **2003.**
3. Wang, L.K.; Chen, J.P.; Hung, Y.; Shammas, N.K.; Heavy Metals in the Environment. CRC Press, Boca Raton, USA., **2009.**
4. Nawaz, B.H.; Khadim, R.; Hanif, M.A.; *Iran. J. Chem. Chem. Eng.*, **2011**, *30*, 81–88.
5. Saygideger, S.; Gulnaz, O.; Istifli, E.S.; Yucel, N.; *J. Hazard. Mater.*, **2005**, *126*, 96–104.
6. Maresova, J.; Hornik, M.; Pipiska, M.; Augustin, J.; *Nova. Biotechnol.*, **2010**, *10*, 53–61.
7. Prigione, V.; Zerlottin, M.; Refosco, D.; Tigini, V.; Anastasi, A.; Varese, G.C.; *Bioresour. Technol.*, **2009**, *100*, 2770–2776.
8. Prabakaran, R.; Arivoli, S.; *Eur. J. Appl. Eng. Sci. Res.*, **2012**, *1*, 134–142.
9. Demirbas, A; *J. Hazard. Mater.*, **2008**, *157*(2–3), 220–229.
10. Loukidou, M.X.; Zouboulis, A.I.; Karapantsios, T.D.; Matis, K.A.; *Colloids Surf. A.*, **2004**, *242*, 93-104.
11. Shukla, A.; Zang, Y.H.; Dubey, P.; Margrave, J.L.; Shukla, S.S.; *J.Hazard. Mater.*, **2002**, *95*, 137-152.
12. Argun, M.E.; Dursun, S.; Ozdemir, C.; Karatas, M.; *J. Hazard. Mat.*, **2007**,*141*, 77-85.
13. Laszlo J.A.; Dintzis F.R.; *J. Appl. Polym. Sci.,* **1994**, *52*(4), 531–538.
14. Osman H.E.; Badwy R.K.; Ahmad H.F.; *J. Phytol.*, **2010**, *2*, 51–62.
15. Liang, J.; Li, X.; Yu, Z.; Zeng, G.; Luo, Y.; Jiang, L.; Yang, Z.; Qian, Y.; Wu, H.; *Sustainable Chem. Eng.*, **2017**, *5*, 5049–5058.
16. Yu, L.J.; Shukla, S.S.; Dorris, K.L.; Shukla, A.; Margrave, J.L.; *J. Hazard. Mater.* B., **2003**, *100*, 53–63.
17. Reddy, D.H.K.; Harinath, Y.; Seshaiah, K.; Reddy, A.V.R.; *Chem. Eng. J.*, **2010**, *162*, 626-634.
18. Yuvaraja, G.; Krishnaiah, N.; Subbaiah, M.V.; Krishnaiah, A.; *Colloids Surf.* B., **2014**, *114*, 75-81.
19. Athar, M.; Farooq, U.; Aslam, M.; Salman, M.; *Appl. Water Sci.*, **2013**, *3*, 665–672.
20. Sing, C.; Yu, J.; *Water Res.*, **1988**, *32*, 2746.
21. Hassan, M.M.; Yasin, M.M.; Yousra, M.; Ahmad, R.; Sarwar, S.; *Environ. Sci. Pollut. Res.,* **2018**, *25*(13), 12570-12578.
22. Bhatnagar, A.; *J. Hazard. Mater.* B., **2007**, *139*, 93-102.
23. Ho, Y. S.; Mckay, G.; Wase, D.J.; Foster, C.F.; *Adsorpt. Sci. Technol.*, **2000**, *18*, 639-650.
24. Lim, J.; Kang, H.M.; Kim, L.H.; Ko, S.O.; *Environ. Eng. Res.*, **2008**, *13*(2), 79-84.
25. Cordero, B.; Lodeiro, P.; Herrero, R.; de Vicente, M.E.S.; *Environ. Chem.*, **2004**, *1*, 180–187.
26. Kalavathy, M.H.; Karthikeyan, T.; Rajgopal, S.; Miranda, L.R.; *J. Coll. Interf. Sci.*, **2005**, *292*, 354-362
27. Mckay, G.; Otterburn, M.S.; Sweeney, A.G.; *Water Res.*, **1980**, *14*, 15–20.
28. Bazargan-Lari, R.; Zafarani, H.R.; Bahrololoom, M.E.; Nemati, A.; J. *Taiwan Institute Chem. Eng.*, **2014**, *45*, 1642–1648.
29. Meitei, M.D.; Prasad, M.N.V.; *Ecol. Eng.*, **2014**, *71*, 308–317.
30. Lee, S.Y.; Choi, H.J.; *J. Environ. Manag.,* **2018**, *209*, 382-392.
31. Ghomri, F.; Lahsini, A.; Laajeb, A.; Addaou, A.; Larhyss J, 2013, 37–54
32. Ihsanullah; Abbas, A.; Al-Amer, A.M.; Laoui, T.; Al-Marri, M.J.; Nasser, M.S.; Khraisheh, M.; Atieh, M.A.; *Sep. Purif. Technol.,* **2016**, *157*, 141–161.
33. Leudjo, T.A.; Pillay, K.; Mbianda X.Y.; *Emerging trends in chemical sciences.*, **2018**, 313–343.
34. Ahmad, M.A.; Puad, A.; Azreen, N.; Bello; Solomon, O.; *Water Resour. Ind.*, **2014**, *6*, 18–35.
35. Javed, M.A.; Bhatti, H.N.; Hanif, M.A.; Nadeem, R.; *Sep. Sci. Technol.*, **2007**, *42*, 3641–3656.